International Journal of Mechanical, Industrial and Aerospace Sciences
ISSN: 2517-9950
Vol:11, No:8, 2017

High-Fidelity 1D Dynamic Model of a Hydraulic Servo Valve Using 3D Computational Fluid Dynamics and Electromagnetic Finite Element Analysis

D. Henninger, A. Zopey, T. Ihde, C. Mehring

***Abstract*—**The dynamic performance of a 4-way solenoid operated hydraulic spool valve has been analyzed by means of a one-dimensional modeling approach capturing flow, magnetic and fluid forces, valve inertia forces, fluid compressibility, and damping. Increased model accuracy was achieved by analyzing the detailed three-dimensional electromagnetic behavior of the solenoids and flow behavior through the spool valve body for a set of relevant operating conditions, thereby allowing the accurate mapping of flow and magnetic forces on the moving valve body, in lieu of representing the respective forces by lower-order models or by means of simplistic textbook correlations. The resulting high-fidelity one-dimensional model provided the basis for specific and timely design modification eliminating experimentally observed valve oscillations.

***Keywords*—**Dynamic performance model, high-fidelity model, 1D-3D decoupled analysis, solenoid-operated hydraulic servo valve, CFD and electromagnetic FEA.

I. Introduction

DESPITE the increased availability and affordability of high-performance computing, one-dimensional (1D) modeling based on empirical data and/or simplistic analytical considerations remains an important tool in the product development process of a wide range of engineering applications, including hydraulic systems and components. Areas of use include, trade studies during preliminary design, troubleshooting during qualification testing, and design optimization during the detailed design phase. One reason for the persistence of 1D modeling tools lies in their comparatively short analysis turn-around time specifically in context of large, complex (multi-physics) systems or if a large number of design configurations are to be analyzed.

A fully coupled approach (co-simulation) combining 1D (ODE type) and 3D (PDE type) models concurrently in one simulation, is beneficial to predict dynamic system behavior for cases where local transient physics details (e.g., within a subsystem component) have a decisive effect on overall system behavior, or where boundary conditions to predict detailed subsystem behavior via 3D modeling are dynamic in nature, requiring at least some level of higher-level system modeling via a 1D approach. For example, in [1], the authors present a CFD modelling and simulation environment designed to integrate seamlessly with large-scale system level simulation tools. Reference [2] addresses numerical efficiencies of 1D/3D co-simulation in context of modeling an urban solar thermal system using ANSYS CFD and Modelica software. The effectiveness of 1D/3D co-simulation with focus on the data exchange strategy between 1D and 3D analysis tools is addressed in [3] for the simulation of an aircraft ECS system (using the 1D system simulation tool AMESim) in conjunction with the airflow and temperature behavior in the aircraft cabin (using the CFD solver FLUENT). Details of the coupling methodology between 1D and 3D simulation tools are also discussed in [5] for the flow behavior inside a closely coupled catalytic converter (leveraging the 1D engine simulation code Ricardo WAVE and the 3D CFD Solver STAR-CD) and in [4] from a more general perspective, i.e., the generic coupling of different 1D system and 3D CFD simulation tools via a Mesh-based parallel Code Coupling Interface (MpCCI).

In the framework of a fully-coupled 1D/3D co-simulation approach, CPU time for the analysis is determined by the available computational resources as well as the shortest characteristic time of the relevant physical phenomena to be resolved. In the case of fluid systems, this constraint is often governed by the execution of the Computational Fluid Dynamics (CFD) flow solver producing a time-accurate spatial resolution of local flow behavior. Consequently, co-simulation loses one of the benefits of a pure 1D modeling approach, i.e. short analysis execution time. Naturally, if time-scales of the behavior modeled via the 1D model and those modeled via 3D analysis (e.g., 3D CFD or EM Electromagnetics) are very dissimilar, separate time-stepping between 3D and 1D simulation can be deployed with information being passed between the models only at intermediate time steps. In the limit case, quasi-steady comprehensive 3D analysis to describe, for example, the complex structure of electromagnetic fields, fluid flow fields and their forces for a set of preselected operating conditions can be used in context of the development of a highly accurate 1D dynamic model of the component or system in which these phenomena occur. Development of the prescribed 1D dynamic model can be accomplished in phases, starting with simplistic

D. Henninger, A. Zopey and T. Ihde are with Parker Aerospace, Irvine CA 92606 USA (e-mail: daniel.henninger@parker.com, ashok.zopey@parker.com, thomas.ihde@parker.com).

C. Mehring is with Parker Aerospace, Irvine CA 92606 USA and the Department of Aerospace and Mechanical Engineering, University of California Irvine 92697 (e-mail: carsten.mehring@parker.com).

sub-models that use only empirical or textbook information in the description of complex physical phenomena and their effect, such as electromagnetic and/or fluid forces, for example. As detailed analysis results become available from concurrently carried out quasi-steady simulations of the relevant complex physics phenomena, generic or simplistic behavior/ performance models are replaced by more accurate descriptions of the prevalent physics and their effects. Clearly, 1D and 3D models can be developed concurrently allowing stepwise improvements to the 1D model as 3D model results become available. This parallel-path approach provides notable advantages, especially in the case of component failure analysis and resolution. The authors have pursued this approach in prior work for the case of a fluid-force driven valve [6].

The present work extends the authors' prior work [6] to include electromagnetic forces in their modeling approach and in context of analyzing a direct acting solenoid driven spool valve, as shown in Fig. 2. The aim was to develop a high fidelity 1D dynamic model of the valve in order to understand oscillatory valve behavior during valve-opening, and, through targeted design changes, modify the valve to eliminate those oscillations. It should be noted here that, valve oscillatory behavior results due to minute changes in the force balance on the moving valve body. As such, accurate prediction of the acting magnetic and fluid forces is crucial in order to understand and remedy oscillatory behavior. The same is true for additionally acting forces such as damping forces which form part of the 1D dynamic model but remain challenging to capture accurately. The latter is also true for frictional forces, which have been neglected within the present study.

To develop the prescribed high fidelity model, detailed quasi-steady CFD analyses have been carried out for various spool positions and pressure conditions, thereby allowing the accurate mapping between a given set of valve operating conditions and the resulting fluid forces on the spool. A similar mapping has been carried out for the electromagnetic forces acting on the plunger (connected to the spool) as a function of both the current through the solenoids and the plunger position. CFD analyses have been carried out for incompressible flow using ANSYS CFX v.16.2 and deploying its Reynolds Averaged Navier-Stokes (RANS) model together with its SST turbulence model. The potential for cavitation onset was not considered in these analyses. Company internal and industry-wide best practices for CFD [2] were followed to assure accuracy of the 3D analysis results.

To resolve the 3D electromagnetic fields generated by the solenoids and the resulting magnetic forces acting on the plunger, the commercial software package MagNet v7.4 by Infolytica was employed.

II. Valve Operation and Geometry

The present analysis considers an Electro-Hydraulic-Servo-Valve (EHSV) as shown in Figs. 1 and 2. The motion of the valve is controlled by two linear solenoids. When solenoid #1 is energized, the plunger/spool moves such that the supply pressure (P_{supply}) is connected to the extend side of the actuator port (P_{extend}) and the retract side of the actuator ($P_{retract}$) is connected to return pressure (P_{return}). In this condition, the actuator piston moves to the right in the extend direction against external load (see Figs. 1 and 2). The exact opposite happens when solenoid #2 is energized.

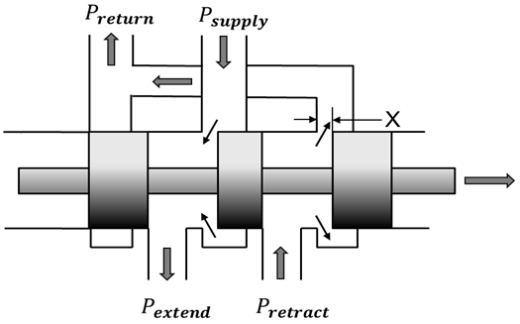

Fig. 1 Detail of spool shown in Fig. 2 [7]

The speed of the actuator is controlled by the effective flow area of the servo valve (extend and retract), piston area, external load, and the magnitude of supply/return pressure (see Fig. 1). In a closed loop position control system the actuator stroke can be controlled by sensing its position (via LVDT) and comparing it to the commanded position, the resulting error signal can be used to send a current command to either solenoid (see Fig. 2). The sign of the error signal determines which solenoid is energized, while the magnitude of the error determines the valve opening. The actuator velocity is proportional to the magnitude of the error signal, i.e. when the actuator position is away from the commanded position, the actuator moves faster than when the actuator position is closer to its commanded position. When the commanded position is reached, both solenoids are de-energized.

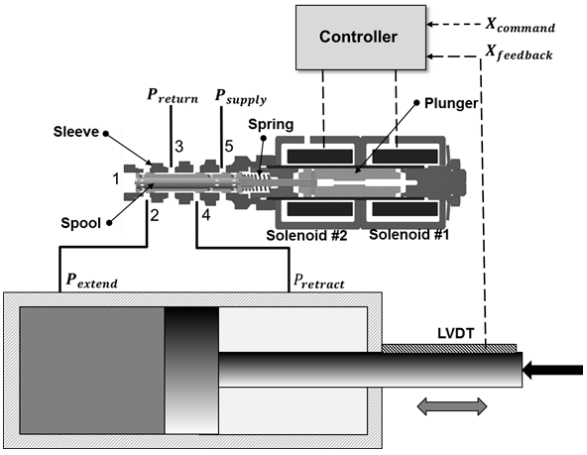

Fig. 2 Solenoid-driven spool valve geometry and schematic

III. Modeling

A. 1D Dynamic Model

The dynamic behavior of the valve can be described by applying Newton's second law to the motion of the spool:

$$m\frac{d^2x}{dt} = F_{solenoid} + F_{fluid} - F_{preload} - K_{spring}x - C\frac{dx}{dt} \quad (1)$$

where m denotes the effective mass (i.e. mass of spool, solenoid plunger and spring), $F_{solenoid}$ is the force exerted by the solenoid, F_{fluid} represents the sum of all fluid forces exerted on the spool, $F_{solenoid}$ is the force exerted by the preloaded spring on the spool, K_{spring} is the spring rate, and C is the viscous damping coefficient.

The force generated by the solenoid is a function of the current, the position of the plunger. A series of force-vs-stroke curves at various values of constant current are developed using the magnetic FEA software MagNet 7.4 (by Infolytica).

Within previous 1D modeling approaches, fluid forces and valve effective flow areas have been determined based on first principles, published literature or from test data. Due to the sensitivity of the present valve design on electromagnetic forces, fluid forces and the effective flow area, CFD and EM FEA analysis has now been deployed to determine spool fluid forces, effective flow areas, and electromagnetic forces. The fluid forces are described as functions of the non-dimensional force coefficient C_f and effective flow area Ae, i.e.

$$C_f = \frac{F_{fluid}}{A_{ref}\, dP} \quad (2)$$

$$Ae = \frac{Q}{\sqrt{2\frac{dP}{\rho}}} \quad (3)$$

where F_{fluid} is the fluid force on the spool, Q is the volumetric flow rate through the ports, ρ represents the hydraulic fluid density, dP is the difference in port pressures, and A_{ref} is an arbitrary reference area chosen to be 1 mm^2. The values of C_f and Ae were derived from 3D CFD analyses assuming steady-state conditions. The implication of this assumption is that these coefficients are strictly only applicable for conditions where transient fluid phenomena are relevant. For the purpose of characterizing, the present servo valve these limitations did not impose a concern. Fig. 3 shows the implementation of the coefficient and force values into the 1D model.

The pressures in the nodal volumes used in the 1D model were calculated from the consideration of inflow and outflow from the prescribed control volumes and the rate of change of that volume, taking into account fluid compressibility. While the force and flow coefficients are based on steady-state analysis, the upstream/downstream pressures and the spool position are all calculated dynamically. For example, as flow leaves a fixed volume, the pressure will decay with time according to the bulk modulus of the fluid. The lines from pump and reservoir to various ports are simulated, with consideration of fluid inertia effects.

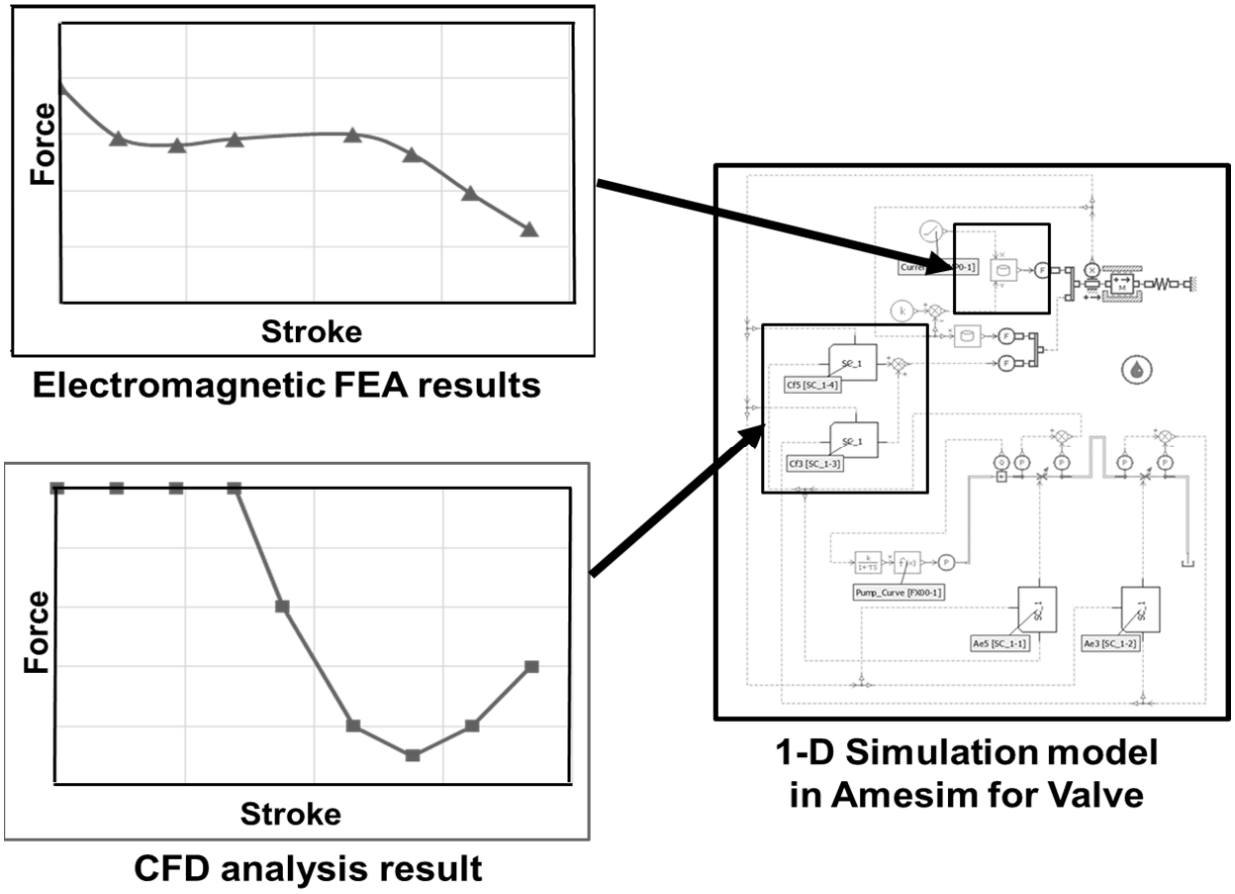

Fig. 3 Incorporation of the look-up tables generated by CFD and EM FEA into the 1D model

Amesim ver. 15 was used to model the valve and system test setup for the 1D simulation (see Fig. 4). The model includes the use of the mechanical library, the hydraulic library, and the signals library available within Amesim. The mechanical components model the 1D dynamics of the valve based on the net instantaneous force acting on the valve, the hydraulic components model the dynamics of the fluid circuit, and the signal components model the interaction between them along with the implemented lookup tables.

The 1D model is based on the test setup shown in Fig. 12. The inlet to the line leading to Port 5 is modeled with a lookup table for the pump supply pressure as a function of flow rate. A short time-duration lag is introduced between the flow rate sensor and the pump to prevent an implicit calculation. Variable orifices are used for the port flow rate calculations, where the flow area of the orifices is determined by a 2D lookup table as a function of the stroke of the spool and the pressure drop across the port. Another input to the model is the current, which varies linearly from 0 to 1.5 amperes over 15 seconds.

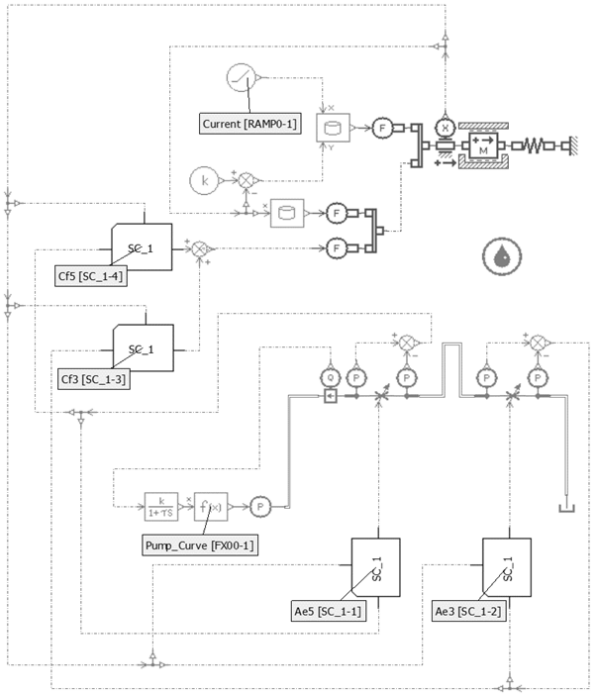

Fig. 4 Schematic of the employed 1D Amesim model

B. 3D CFD and Electromagnetic FEA

The steady-state CFD analysis was run for a combination of various spool positions and boundary conditions. The total-pressure boundary conditions were determined by the pressures measured at each of the ports during testing (see Fig. 12). In the region of oscillatory valve behavior, the pressure at each port was varying (see Fig. 13), so the CFD analysis was performed at boundary conditions which reflect the maximum and minimum pressures recorded (see Fig. 5). Since the path from Port 5 to 2 is isolated form the path from port 4 to 3, the fluid force acting the spool through each path could be calculated independently, thereby reducing the number of CFD cases to be analyzed.

The CFD mesh was regenerated for each spool position, with a typical mesh size of 8.5 million elements, and the spool position ranging from 0.57 mm (when the port just starts to open) to 2.1 mm (when the spool hits the stop). A total of 15 positions were analyzed, with a higher proportion of cases analyzed in the oscillatory region.

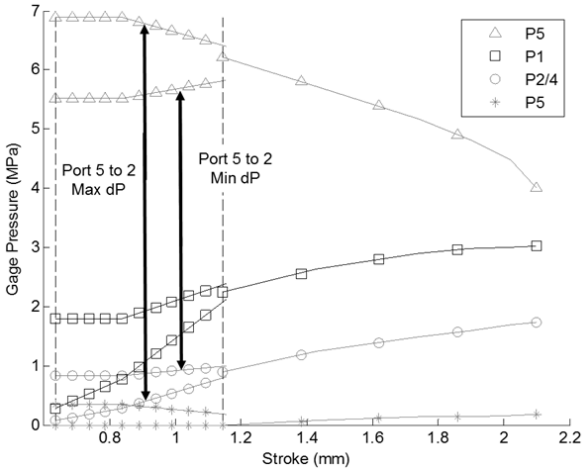

Fig. 5 Pressure boundary conditions used at each port. Each marker represents a CFD analysis case

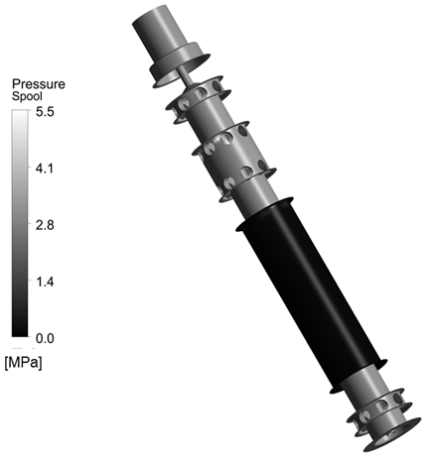

Fig. 6 Wetted surface of the spool for force calculation

The force on the spool and the mass flow rate through the ports were extracted from the CFD analysis results at the given boundary conditions and spool stroke. To obtain the force on the spool, the wetted spool surfaces were combined into one surface (see Fig. 6), and the sum of forces acting on this surface in the axial direction was automatically calculated by the software. The spool surface for the flow path from port 5 to 2 was isolated from the flow-path surface connecting port

4 to 3. This allowed for a force coefficient to be determined for each flow path, and when used in the dynamic model these coefficients determine the force contribution from each path due to the instantaneous pressures at each port.

The force coefficients for each of the flow paths can be seen in Fig. 8. A positive value of C_f represents a force that acts to open the valve, while a negative value acts to close the valve. At low strokes in the region of oscillations, a coefficient is displayed at both the minimum *dP* boundary condition and the maximum *dP* condition (see Fig. 5). The lookup table in the 1D model linearly interpolates between these two values when the instantaneous *dP* lies between those extremes.

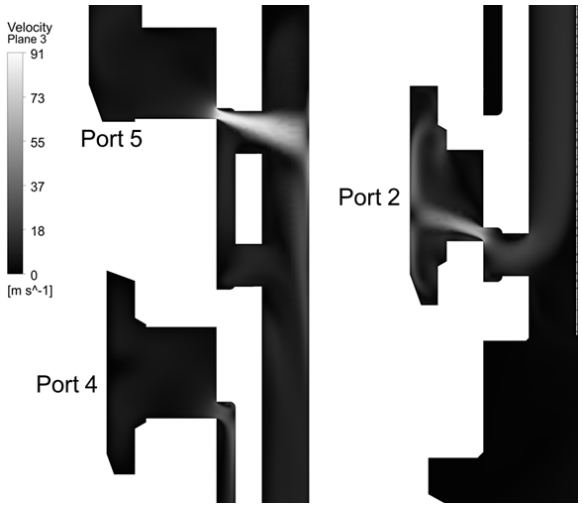

Fig. 7 Expanded view of the spool flow area with ports specified as shown in Fig. 2. Shown are velocity contours from CFD analysis results

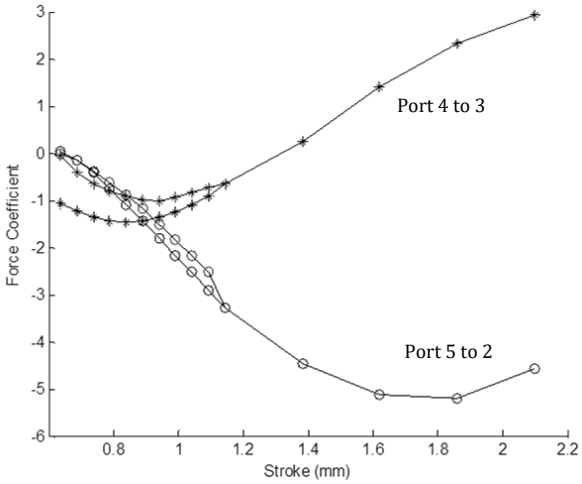

Fig. 8 Force coefficient for both of the flow paths obtained from CFD analysis

The effective flow areas for both flow paths are shown in Fig. 9. Notably, the flow path from Port 4 to 3 opens before the path between Port 5 to 2 is open to flow, which can be verified visually by inspecting the valve hardware.

The electromagnetic model was run using the magnetostatic solver in Infolytica MagNet ver. 7.4, which includes the nonlinear behavior of the material B-H curves. The latter were calibrated based on available test force data. The plunger/spool position was varied for each case to get an overall profile of the magnetic force versus plunger position. When changing the plunger position, the analysis model was re-meshed before solving, with an average mesh size of 1.5 million elements and an adequate far field boundary condition. The current through the "pull coil" (Solenoid #1) was varied from 0.18 amperes up to 1.5 amperes, while the "push coil" (Solenoid #2) was kept de-energized. In operation, these two coils are never energized at the same time. For the observed oscillatory behavior, only the prescribed condition ("pull" condition) was relevant.

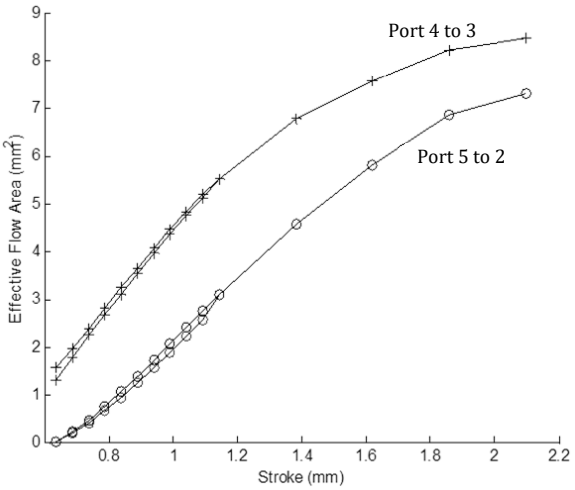

Fig. 9 Effective flow area for both of the flow paths obtained by CFD analysis

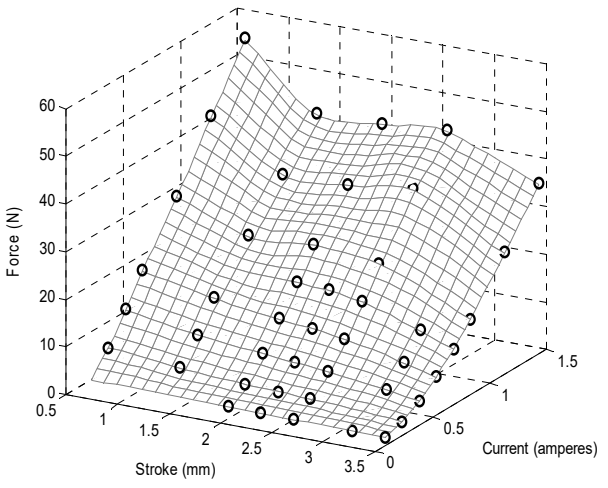

Fig. 10 Magnetic force acting on the plunger/spool as a function of stroke and current obtained by EM FEA

The magnetic force acting on the plunger/spool assembly was extracted from the EM FEA model. A surface map of this

force as a function of plunger position and current is plotted in Fig. 10. This surface map can be directly incorporated into the 1D model without the need for a non-dimensional force coefficient. An example of the flux density is shown in Fig. 11. At this maximum current condition, it can be seen that the flux is saturating in the pole face and the plunger face. Although not presented here, the EM FEA model was also instrumental in evaluating the different force responses between the push and the pull direction. The asymmetry in the design was found to be the main contributor to this difference, namely the flux was saturating in the walls for the "push" direction, which are thinner due to the need for a shaft connecting the plunger and the spool.

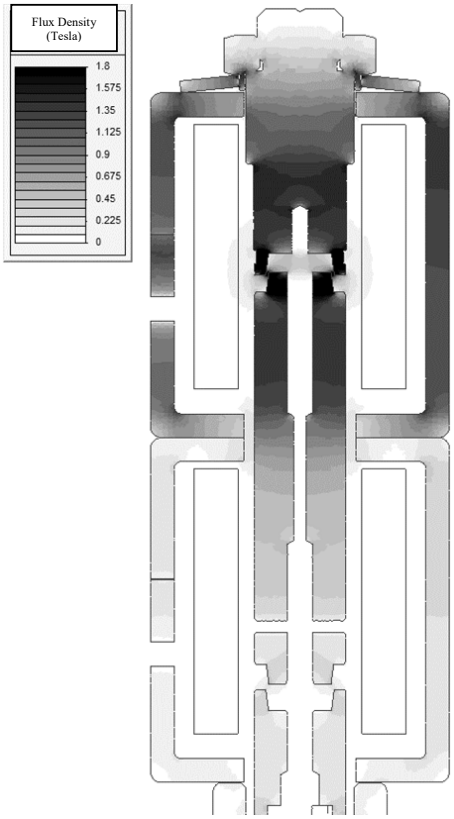

Fig. 11 Flux density contours obtained by EM FEA at maximum current

IV. Results

A schematic of the test setup is shown in Fig. 12. A pump pressurizes the hydraulic fluid from a tank and delivers it to Port 5. Along this line, the pressure and flow rate are measured. When the valve is in the "pull" position (the case when oscillations are observed), the fluid flows from Port 5 to Port 2, Port 2 to Port 4 through a connecting line, and finally from Port 4 to Port 3 and to the tank. The line after Port 1 is deadheaded, preventing any flow from exiting that port.

The dynamic 1D model discussed earlier was able to capture valve oscillations observed experimentally during the initial excitation of the solenoid. These oscillations start immediately after the path from Port 5 to 2 opens. As the current is increased further, the amplitude of the oscillations diminishes and the flow stabilizes throughout the rest of the valve stroke (see Fig. 13). The same stabilizing nature is observed experimentally. When the current is decreased back down to zero, the valve begins to oscillate at about the same current value that it stopped oscillating on the ramp up. This behavior is observed both experimentally and in the simulation.

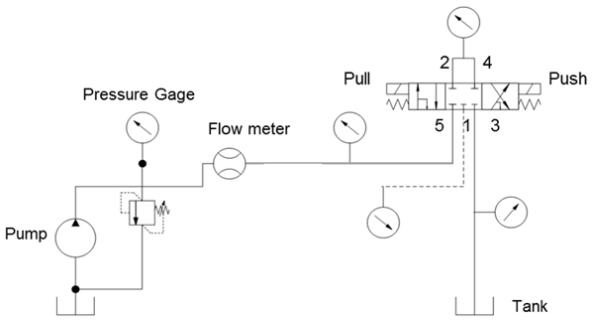

Fig. 12 System schematic of the test setup

The described oscillatory behavior is only observed in the analysis model when the line volumes and line losses are included. These line volumes are significant compared to the volume within the valve cavities. When the 1D model only included the CFD and EM FEA results of the valve, neglecting the flow lines of the system in which the valve was tested, the simulation failed to show oscillations. Even a fully transient 3D CFD and EM FEA study of the valve would likely fail to show the oscillations, unless the lines of the entire system were modeled in CFD, greatly increasing computational time. This highlights a key benefit of using the 1D-3D decoupled simulation approach, i.e. changing the system within which the valve is implemented to investigate its effect on the performance and vice versa.

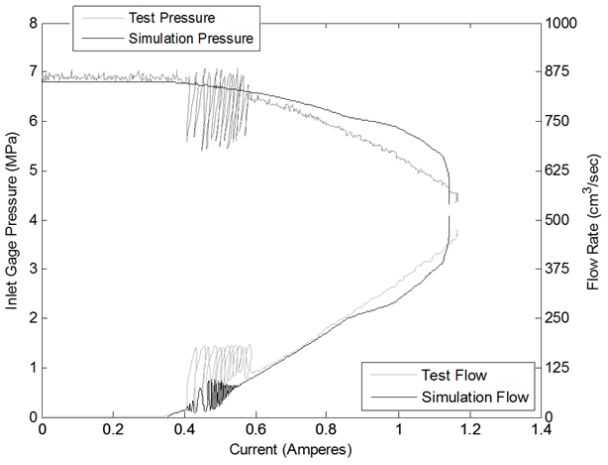

Fig. 13 Simulation and test results showing flow oscillations

An updated spool geometry was analyzed with the 1D

model after updating the relevant fluid flow and force maps by running additional CFD analyses. Both simulation results and test data indicated that the modified geometry provides for significant performance improvements. Simulation results from the final design are shown in Fig. 14 illustrating the complete elimination of the previously observed valve oscillations.

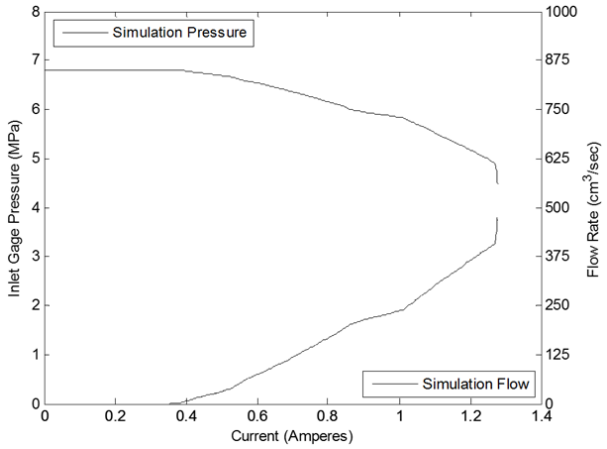

Fig. 14 Simulation results for modified spool geometry

V. Conclusion

A decoupled 1D-3D analysis approach has successfully been employed to describe the dynamic behavior of a direct acting solenoid driven spool valve. Maps of fluid force and electromagnetic force as function of spool/plunger position and dependent on fluid port pressure conditions and solenoid current have been generated using 3D CFD analysis and 3D Electromagnetic FEA analysis. A high-fidelity dynamic 1D model was developed which employed the prescribed force maps. The resulting model identified that valve oscillations observed during operation were related to the hydraulic fluid lines connecting to the valve and inadequate synchronization of the spool lands and/or fluid ports. Design changes suggested by further exercising the 3D and 1D models, resulted in elimination of the observed valve oscillations.

Acknowledgment

The authors would like to thank Dan Waina, Nathan Rosenbaum, and William Guse of Parker Hannifin Hydraulic Cartridge Systems Division for providing funding support for this project and for their input, guidance and active participation during the project execution phase.

References

[1] M. Gayer, J. Kortelainen and T. Karhela, "CFD modeling as an integrated part of multi-level simulation of process plants: semantic modelling approach," *Proc. of the 2010 Summer Computer Sim. Conf. (SCSC '10)*. Society of Computer Simulation International, San Diego, CA, USA, 219-227.

[2] M. Ljubijankic, C. Nytsch-Geusen, A. Jänicke, and M. Schmidt, "Advanced Analysis of Coupled 1D/3D Simulation Models by the Use of a Solar Thermal System," *Proc. of the 12th Conf. of Int. Building Perf. Sim. Association*, 2011, pp. 1871-1877.

[3] X. Chen, J. Yang, T. Yu, and S. Yang, "A Coupled 1D/3D Co-Simulation Approach in Simulating Aircraft Cabin Temperature Field," Int. J. of Sim. Systems. Science and Technology, Vol.17, No. 40, pp. 11.1-11.7.

[4] K. Wolf, and P. Bayrasy, "Generic Coupling of 1D System Codes with 3D CFD Tools," ERCIM News, 2010, No.81, pp.27-28, ISSN: 0926-4981.

[5] Z. Liu, S., Benjamin, C. Roberts, H. Zhao, and A. Arias-Garcia, "A coupled 1D/3D simulation for the flow behaviour inside a close-coupled catalytic converter," SAE Technical Paper, 2003-01-1875.

[6] C. Mehring, A. Zopey, M. Latham, T. Ihde, and D. Massie, "Decoupled 1D/3D Analysis of a Hydraulic Valve," Int. Conf. of Comp. Methods in Sci. and Eng. 2014, AIP Conf. Proc. 1618, 2014, pp. 979-982.

[7] H. E. Merritt, "Hydraulic Control Systems," John Wiley and Sons, Inc., 1967, Ch. 5, pp. 76-77.